Journal of the Serbian Society for Computational Mechanics / Vol. 17 / No. 2, 2023 / pp 27-37
(10.24874/jsscm.2023.17.02.03)

# NUMERICAL ANALYSIS OF V-SHAPED PROTECTIVE PLATES AT VARIOUS ANGLES SUBJECTED TO BLAST LOADING – A COMPARATIVE ANALYSIS

**Miloš S. Pešić[1*], Aleksandar S. Bodić[2], Živana M. Jovanović Pešić[2], Nikola B. Jović[2] and Miroslav M. Živković[2]**

[1] Institute for Information Technologies, University of Kragujevac, Jovana Cvijica bb, 34000 Kragujevac
e-mail: milospesic@uni.kg.ac.rs
[2] Faculty of Engineering, University of Kragujevac, 6 Sestre Janjić Street, 34000 Kragujevac
e-mail: abodic@uni.kg.ac.rs, zixi90@gmail.com, njovic1995@gmail.com, zile@kg.ac.rs
**corresponding author*

## Abstract

The mechanical response of blast-resistant vehicles, such as Infantry Fighting Vehicles (IFVs), Mechanized Infantry Combat Vehicles (MICVs), Armored Personal Vehicles (APVs), and Mine-Resistant Ambush-Protected (MRAP) vehicles, is crucial for their effective design. When designing armored vehicles, it is important to achieve a balance between rigid designs that transmit blast forces to the troop's cabins and softer designs that prevent excessive structure deformation hazardous to the troops. This study investigates the performance of V-shaped plates at different angles under blast loading. The focus is on modeling blast effects using the Conventional Weapon (ConWep) method and the Johnson-Cook material model. The material used for V-shaped protective plates STRENX700 (S690QL) armor steel is commonly used for blast protection in Anti-Landmine (ALM) Vehicles. The blast-wave induces large deformation, erosion, high strain rates, non-linear material behavior and fragmentation. The numerical simulation results are presented in the form of vertical displacement of the central node on the protective plate, von Mises equivalent stress, and equivalent plastic strain.

**Keywords:** V-Shaped protective plate, finite element method, Johnson-Cook material model.

## 1. Introduction

The magnitude of the threat posed by blast loading on public and military infrastructure is of the highest priority. The troops in armored vehicles are exposed to grave danger, as they face the imminent risk of fatality resulting from blast loading induced by landmines and improvised explosive devices (IEDs). Furthermore, structural components like columns and plates can sustain significant damage from blast loads. Given the multitude of variables involved, including the angle of the V-shaped plate, and the charge's position and configuration, among others, the task of determining the response of an armored vehicle to blast loading becomes a formidable challenge.

The blast wave's impact evaluation on the armored vehicle and its systems plays a crucial role in mitigating vehicle deformation (Sunil Kumar and Schmidova, 2019), thereby enhancing the safety of soldiers inside. The research paper by Mahajan and Muralidharan (2017) justifies the utilization of numerical simulations as a viable approach in armored vehicle design, offering advantages such as reduced number of prototypes and shorter development time. Within numerical simulations, different types and sizes of finite elements can be used in order to achieve accuracy. Convergence is achieved by implementing five distinct mesh densities for modeling the floor and protective plates of the armored vehicle (Pešić et al. 2022). Armored vehicles are equipped with steel plates that safeguard soldiers against explosions. The geometry of the explosive protection plates might vary (Pešić et al. 2022), with V-shaped configurations being extensively examined in papers (Trajkovski et al. 2018; Cong et al. 2021; Markose and Rao 2017). Determining the optimal angle for the V-shaped protective plates holds paramount importance in ensuring minimal acceptable damage to the armored vehicle. Experimental tests of armored vehicles subjected to the blast wave were carried out in Dišić (2018). Also, within this literature, the verification of the obtained experimental results was performed using numerical simulations.

The study for this report was undertaken in accordance with NATO AEP-55 STANAG 4569 Levels 2, 3, and 4. (NATO Standard 2014).

The primary objective of this paper is to ascertain the optimal angle for the V-shaped protective plates. This angle is crucial in minimizing the potential damage inflicted upon the armored vehicle, thereby ensuring the highest level of protection for both soldiers and the vehicle itself against the blast wave generated by anti-landmine (ALM) explosions.

## 2. Problem description and FE models

The utilization of a V-shaped protective plate stands as one of the most effective geometries for providing adequate safeguarding to soldiers, armored vehicles, and military equipment against anti-landmine mines (ALMs) and improvised explosive devices (IEDs). Under the armored vehicle's floor is the hull, which is made of a metal plate and bent into a V shape. The V-shaped hull was modelled in eight different geometries, as shown in Fig. 1, in order to define the best angle. The blast originates from an anti-landmine located directly beneath the V-shaped hull, positioned at a distance of 500 mm, as shown in Fig. 1. The dimensions of V-shaped protective plates are 2 m in width and 3 m in length.

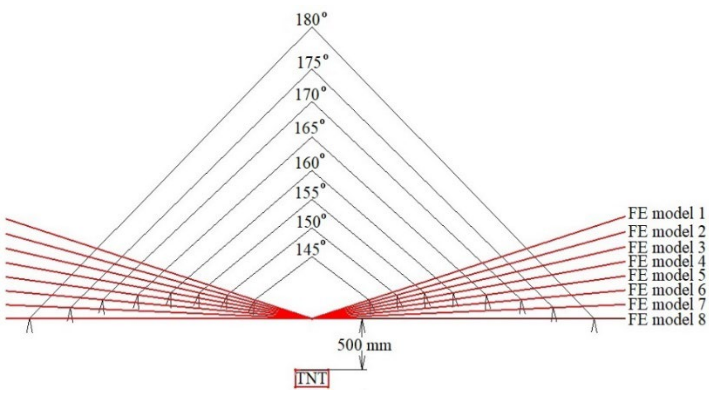


**Fig. 1.** V-shaped protective plate angles

In this study, the V-shaped protective plate is fixed to the floor of the armored vehicle along all four edges. To ensure sufficient strength and durability, an appropriate type of steel material was chosen for the protective plate. Numerical testing was conducted on the V-shaped protective plates to evaluate their ability to withstand blast loading generated by 6 kg, 8 kg, and 10 kg of trinitrotoluene (TNT) placed directly beneath the V-shaped hull. It is known that various factors influence the explosion parameters, such as burial depth, sand composition, explosive shape, and more. However, for the purposes of this research, a simplified model of the explosion was used.

This paper focuses on investigating the significance of the V-shaped protective plate angle in reducing incident explosion waves. The clearance value for all analyzed models remains consistent throughout the study. The TNT masses employed in this research are 6 kg, 8 kg, and 10 kg, respectively. This corresponds to levels 2, 3, and 4 of protection, as defined by the NATO standard (NATO Standard 2014). The thickness of the V-shaped protective plate in all finite element (FE) models is set at 12 mm. The FE model was created in the FEMAP v2021.2 program (FEMAP Theory Manual 2021) using the CAD model, and the input file for the LS-DYNA software (LS-DYNA Theory Manual 2014) was exported thereafter. The LS-DYNA software was used to perform explicit dynamic analysis. Post-processing of the models was also performed in FEMAP v2021.2 software. The floor of the armored vehicle was modelled using 3D hexahedral eight-noded finite elements, while the V-shaped protective plates were modelled using four-noded plate elements, as presented in Fig. 2. The protective plates in all FE models were subjected to a hemispherical incident wave during the analysis. In the FE models, the 3D hexahedral eight-noded finite elements, which are used to model the floor of the vehicle have dimensions of 30 mm x 30 mm x 15 mm, while the four-noded plate elements used for modeling the V-shaped protective plates have dimensions of 30 mm x 30 mm.

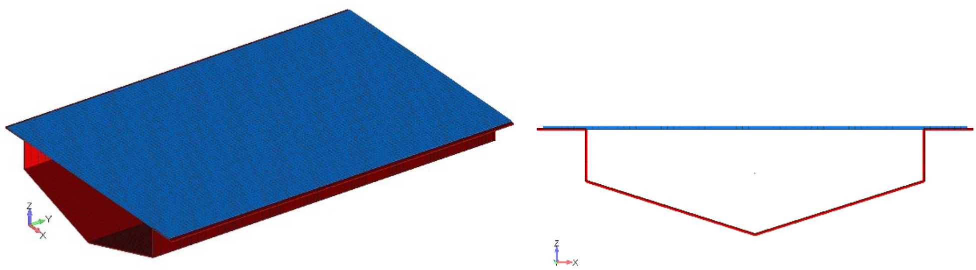


**Fig. 2.** FE model of V-Shaped protective plate

## 3. Blast loading

The explosion process involves a chemical reaction that occurs within a very short time frame, typically within milliseconds. This rapid reaction leads to the high-velocity expansion of the reaction products in an outward direction. This leads to a blast wave generation, propagating outward with a sudden change in various field parameters such as particle velocity, density, pressure, and internal energy across the shock front. The blast wave exerts a significantly higher pressure, denoted as $p_s$, compared to the ambient pressure, denoted as $p_a$. The difference between these pressures is known as blast overpressure, represented as ($p_s$-$p_a$). The blast wave consists of both positive and negative phases, and is shown in Fig. 3. The pressure-time history of a blast wave typically exhibits distinctive characteristics. It consists of a rapid rise in pressure followed by a peak pressure, and then a gradual decay over time. This pattern is commonly referred to as the "Friedlander waveform". The rise time, duration, and decay of the pressure wave can vary depending on the specific explosive, its distance from the point of observation, and the surrounding environment. Generally, the pressure-time history of a blast wave reflects the rapid release of energy during the explosion, leading to the propagation of a high-pressure shock wave that gradually dissipates as it travels away from the source.

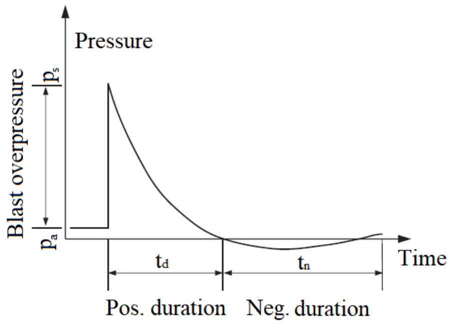


**Fig. 3.** The pressure-time history of a blast wave

The pressure-time history of a blast wave can be mathematically represented by the modified Friedlander equation:

$$p(t) = (p_s - p_a)\left[1 - \frac{t - t_a}{t_d}\right] e^{\frac{-(t-t_a)}{\theta}} \tag{1}$$

In the previous equation $t_a$ represents the time of arrival, which is the point in time when the blast wave reaches a specific location. $t_d$ denotes the duration of the positive phase, which is the period during which the pressure remains above the ambient pressure. θ represents the decay constant, which determines the rate at which the pressure decreases during the decay phase of the blast wave. This equation takes into account various factors that influence the blast wave, such as the distance from the explosion, the size and type of explosive, and the surrounding environment. The modified Friedlander equation provides a model for predicting the temporal behavior of the blast wave's pressure as a function of time. The pressure-time characteristics of blast waves can be analyzed and estimated using this equation, aiding in the design and assessment of various structures and protective measures against explosions.

## 4. Johnson-Cook material model

When considering high strain rates, armor steel is selected as the material for the V-shaped protective plate. Under such conditions, the material undergoes plastic deformation, experiences an increase in temperature, and may ultimately fail due to the blast wave's effects. In numerical simulations, the Johnson-Cook material model is commonly used to simulate temperature and high strain rate effects. The von Mises flow stress in this model can be expressed as follows:

$$\sigma = \left[A + B\varepsilon^n\right]\left[1 + C\ln\dot{\varepsilon}^*\right]\left[1 - T^{*m}\right] \tag{2}$$

The homologous temperature $T^*$ is defined as:

$$T^* = \frac{T - T_0}{T_{melt} - T_0} \tag{3}$$

where, $T$ – represent material temperature, $T_{melt}$ – represent melting point of material and $T_0$ – represent reference temperature (room temperature).

A, B, C, n, and m are material constants and can be calculated using various tests, or by fitting the flow stress data based on static and dynamic tests. The parameter D is used to calculate the material damage initiation and progression. The value of parameter D reflects the accumulated damage in the material. It increases with the strain rate and temperature, based on the material's response to dynamic loading conditions, and is defined as:

$$D = \sum \frac{\Delta \varepsilon}{\varepsilon^f} \tag{4}$$

where, $\Delta\varepsilon$ – represents equivalent plastic strain and $\varepsilon^f$ – represents equivalent strain to fracture.

When the parameter D reaches the value 1 the fracture is occurred. The fracture strain is expressed as:

$$\varepsilon^f = \left[D_1 + D_2 \exp D_3 \sigma^*\right]\left[1 + D_4 \ln \dot{\varepsilon}^*\right]\left[1 + D_5 T^*\right] \tag{5}$$

where, $D_1$-$D_5$ – represent material damage parameters, and where:

$$\sigma^* = \frac{\sigma_m}{\bar{\sigma}} \tag{6}$$

and $\sigma_m$ – represent average normal stress and $\bar{\sigma}$ - represent the von Mises equivalent stress.

Several varieties of armored steel exhibiting varying levels of ductility and strength are available for selection. For this analysis, a steel type with a moderate level of ductility and sufficient strength has been chosen. This selection is based on the understanding that ductility plays a crucial role in dissipating energy during blast loading scenarios. Steel chosen for protective plates within numerical simulations is S690QL which, due to its increased strength, exhibits significantly higher stiffness when subjected to blast loading. The Johnson-Cook material characteristics of S690QL are given in Table 1.

| **Parameter** | **Value** |
|---|---|
| Density $\rho$ [t/mm$^3$] | 7.85E-9 |
| Young's modulus $E$ [MPa] | 228368.9 |
| Poisson's ratio ν [-] | 0.3 |
| Yield stress $A$ [MPa] | 767.38 |
| Proportionality coefficient $B$ [MPa] | 445.13 |
| Reinforcement exponent $n$ [-] | 0.5075 |
| Strain rate Impact parameter $C$ [-] | 0.0265 |
| Temperature Impact parameter $m$ [-] | 1.354 |
| Damage parameter $D_1$ [-] | 120 |
| Damage parameter $D_2$ [-] | 0.645 |
| Damage parameter $D_3$ [-] | 0.065 |
| Damage parameter $D_4$ [-] | 0.120 |
| Damage parameter $D_5$[-] | 3 |

**Table 2.** Johnson-Cook material parameters for S690QL (Dišić, 2018)

The material parameters given in Table 1 were taken from Dišić (2018) in which they were determined through experimental testing conducted on the split Hopkinson tension bar (SHTB).

## 5. Results and discussion

The primary objective of this paper was to determine the most effective geometry for anti-mining protection by comparing the results obtained from explicit dynamic analysis of all eight FE models. Each FE model was subjected to simulated TNT detonations with varying weights: 6 kg, 8 kg, and 10 kg, corresponding to protection levels 2, 3, and 4, as specified in the NATO AEP-55 STANAG 4569 standard.

The numerical simulation results are presented in the form of the maximum vertical displacement of the central node on the protective plate, which is located on the longitudinal plane of symmetry and perpendicular to the protective plate, the maximum value of the von Mises equivalent stress, and the maximum value of plastic deformation for each FE model.

In Table 2, values are presented of the maximum vertical displacement of the central node on the protective plate, the maximum von Mises stress, and plastic deformation for all eight FE models.

| FE model | TNT – 6 kg | | | TNT – 8 kg | | | TNT – 10 kg | | |
|---|---|---|---|---|---|---|---|---|---|
| | T3 (m) | σ (MPa) | ε (-) | T3 (m) | σ (MPa) | ε (-) | T3 (m) | σ (MPa) | ε (-) |
| ID 1 | 0.10 | 977.8 | 0.036 | 0.15 | 1029.2 | 0.086 | 0.23 | 1108.4 | 0.179 |
| ID 2 | 0.13 | 987.8 | 0.043 | 0.21 | 1079.2 | 0.136 | 0.27 | 1124.1 | 0.218 |
| ID 3 | 0.18 | 1026.2 | 0.073 | 0.24 | 1076.8 | 0.145 | 0.27 | 1095.7 | 0.170 |
| ID 4 | 0.20 | 1024.3 | 0.074 | 0.23 | 1048.5 | 0.099 | 0.26 | 1065.9 | 0.115 |
| ID 5 | 0.19 | 993.6 | 0.037 | 0.22 | 997.9 | 0.044 | 0.25 | 1012.5 | 0.054 |
| ID 6 | 0.17 | 957.4 | 0.019 | 0.20 | 977.8 | 0.032 | 0.24 | 992.9 | 0.039 |
| ID 7 | 0.14 | 959.1 | 0.026 | 0.18 | 988.9 | 0.045 | 0.23 | 1004.6 | 0.056 |
| ID 8 | 0.12 | 957.8 | 0.024 | 0.16 | 1007.8 | 0.043 | 0.21 | 1048.4 | 0.081 |

**Table 2.** Numerical analysis results for all eight FE models.

The diagram in Fig. 4 presents the maximum values of vertical displacement for the central node on the protective plate, which is located on the longitudinal plane of symmetry and perpendicular to the protective plate, under a simulated TNT mass of 6 kg.

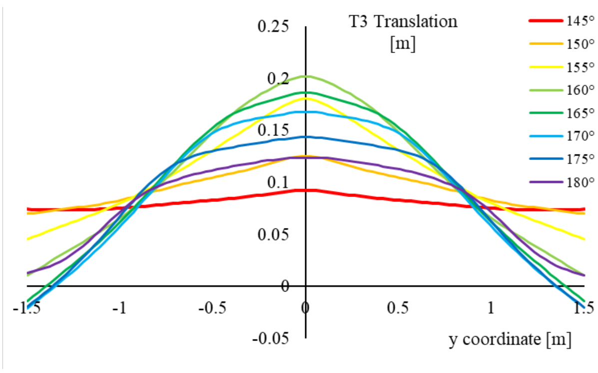


**Fig. 4.** The values of vertical displacement for the central node on the protective plate, obtained from all eight FE models under blast loading conditions with a TNT mass of 6 kg

Based on the results presented in Table 2 and the diagram in Fig. 4, it can be deduced that FE models with the smallest angle (ID 1 - 145°) and the largest angle (ID 8 - 180°) exhibit the least vertical displacement, indicating higher stiffness in these geometries. Additionally, FE models with angles (ID 2 - 150°) and (ID 7 - 175°) also demonstrate high stiffness, as their vertical displacement values are relatively small.

Regarding von Mises stress values, FE models with angles (ID 1 - 145°), (ID 6 - 170°), (ID 7 - 175°), and (ID 8 - 180°) exhibit the lowest stress levels, suggesting superior stress distribution and potential for improved structural integrity. Specifically, FE model (ID 6 - 170°) demonstrates the smallest von Mises stress, with a value of 957.35 MPa, signifying excellent stress resistance. The numerical analysis indicates that FE models with angles (ID 1 - 145°), (ID 6 - 170°), (ID 7 - 175°), and (ID 8 - 180°) possess favorable characteristics, including minimal vertical displacement, high stiffness, and lower von Mises stress values.

The diagram in Fig. 5 presents the maximum values of vertical displacement for the central node on the protective plate, which is located on the longitudinal plane of symmetry and perpendicular to the protective plate, under a simulated TNT mass of 8 kg.

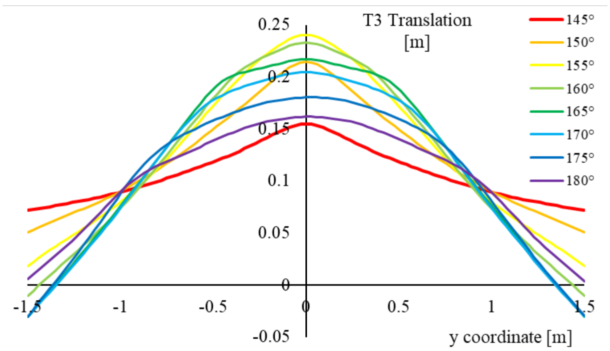


**Fig. 5.** The values of vertical displacement for the central node on the protective plate, obtained from all eight FE models under blast loading conditions with a TNT mass of 8 kg

Based on the results presented in Table 2 and the diagram in Fig. 5, it can be deduced that FE models with the smallest angle (ID 1 - 145°) and the largest angle (ID 8 - 180°) demonstrate the smallest values of vertical displacement, indicating higher stiffness in these configurations. Additionally, FE model (ID 7 - 175°) also exhibits high stiffness, as evident from its relatively small vertical displacement value.

Regarding von Mises stress values, FE models with angles (ID 5 - 165°), (ID 6 - 170°), (ID 7 - 175°), and (ID 8 - 180°) display the lowest stress levels, indicating favorable stress distribution and potential for enhanced structural integrity. Particularly noteworthy is FE model (ID 6 - 170°), which boasts the smallest von Mises stress value of 977.83 MPa, signifying superior stress resistance. The numerical analysis indicates that FE models with angles (ID 1 - 145°), (ID 5 - 165°), (ID 6 - 170°), (ID 7 - 175°), and (ID 8 - 180°) exhibit desirable characteristics, including minimal vertical displacement, high stiffness, and lower von Mises stress values.

The diagram in Fig. 6 presents the maximum values of vertical displacement for the central node on the protective plate, which is located on the longitudinal plane of symmetry and perpendicular to the protective plate, under a simulated TNT mass of 10 kg.

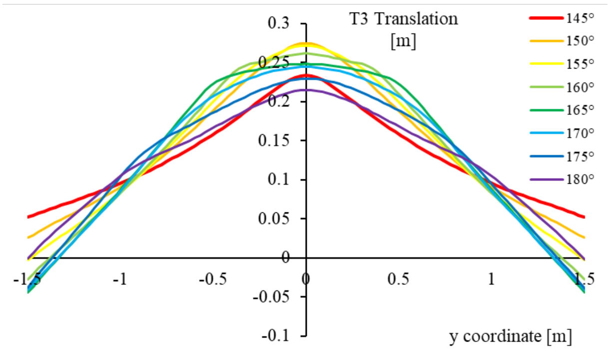


**Fig. 6.** The values of vertical displacement for the central node on the protective plate, obtained from all eight FE models under blast loading conditions with a TNT mass of 10 kg

Based on the results presented in Table 2 and the diagram in Fig. 6, it can be concluded that FE models with the smallest angle (ID 1 - 145°) and the largest angles (ID 7 - 175° and ID 8 - 180°) exhibit the least vertical displacement, indicating higher stiffness in these geometries. Conversely, FE models with angles (ID 2 - 150°) and (ID 3 - 155°) demonstrate the highest vertical displacement values, signifying relatively lower stiffness. Regarding von Mises stress values, FE models with angles (ID 5 - 165°), (ID 6 - 170°), and (ID 7 - 175°) display the lowest stress levels, indicating favorable stress distribution and potential for enhanced structural integrity. Notably, FE model (ID 6 - 170°) exhibits the smallest von Mises stress value of 992.86 MPa, representing superior stress resistance among all models.

The numerical analysis indicates that FE models with angles (ID 1 - 145°), (ID 5 - 165°), (ID 6 - 170°), (ID 7 - 175°), and (ID 8 - 180°) demonstrate desirable characteristics, including minimal vertical displacement, high stiffness, and lower von Mises stress values.

Fig. 7 present the vertical displacement of the central node on the protective plate for FE Model 6 (the most favorable geometry of the V-Shaped plate, based on the results from Table 2) under blast loading conditions with a simulated TNT weight of 8 kg. Vertical displacement provides valuable information about the structural response of the protective plate to the explosive forces, highlighting the areas of maximum deformation and aiding in the assessment of the model's performance under the specified blast scenario.

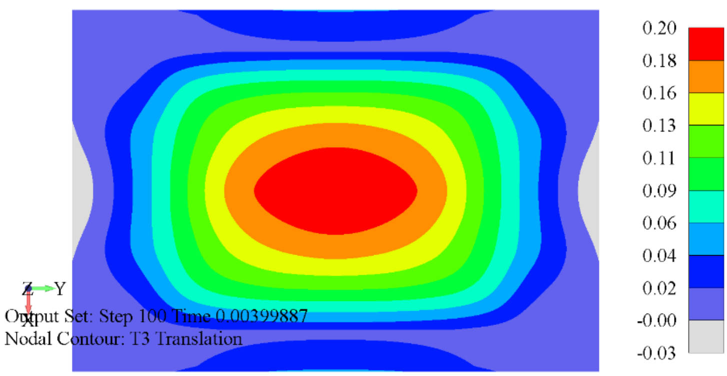


**Fig. 7.** Vertical displacement distribution

Fig. 8 displays the distribution of Von Mises equivalent stress for FE Model 6 (the most favorable geometry of the V-Shaped plate, based on the results from Table 2) under blast loading conditions with a simulated TNT weight of 8 kg. Von Mises equivalent stress distribution offers critical insights into how the protective plate's material is subjected to stress throughout its structure due to the explosive forces. By visualizing the areas of higher stress concentration, this plot aids in evaluating the structural integrity and potential failure points of the protective plate under the specified blast scenario.

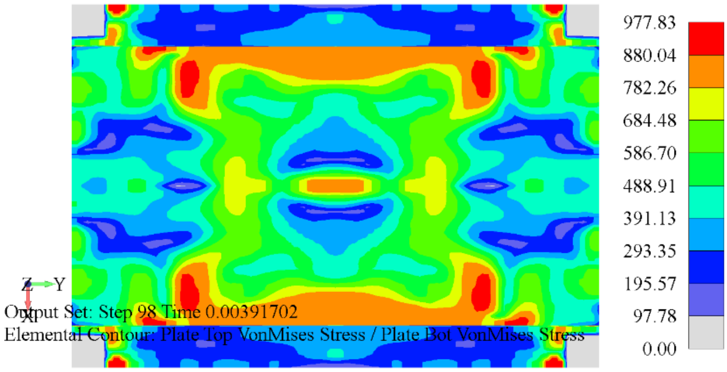


**Fig. 8.** Von Mises equivalent stress distribution

Fig. 9 presents the distribution of plastic strain field for FE Model 6 (the most favorable geometry of the V-Shaped plate, based on the results from Table 2) under blast loading conditions with a simulated TNT weight of 8 kg. This plastic strain field plot provides valuable insights into the areas of significant plastic deformation within the protective plate, indicating regions that have undergone non-recoverable changes in shape or dimensions due to the applied explosive forces. Understanding the plastic strain distribution is crucial for assessing the potential for material failure and determining the structural performance of the protective plate under the specified blast scenario.

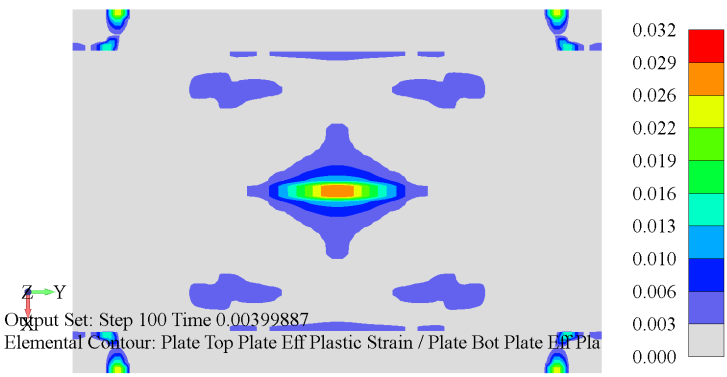


**Fig. 9.** Plastic strain field distribution

## 5. Conclusions

Numerical analysis conducted in this paper aims to investigate the mechanical response of V-shaped protective plates with different angles when subjected to blast loading. The main objective is to determine the optimal angle for these protective plates, which can be effectively utilized in various military vehicles, including Infantry Fighting Vehicles (IFVs), Mechanized Infantry Combat Vehicles (MICVs), Armored Personal Vehicles (APVs), or Mine-Resistant Ambush-Protected (MRAP) vehicles.

Based on the performed FEM numerical analysis, the following conclusions are reached, primarily based on the maximal values of vertical displacement of the central node on the protective plate, the maximal values of von Mises equivalent stress, and maximal values of plastic strain:

- Generally, the maximal vertical displacement of the protective plate increases with higher TNT masses, indicating a greater response to increased blast forces.
- The maximal von Mises equivalent stress also increases with higher TNT masses, signifying higher stress levels experienced by the protective plate under more intense blast loading conditions.
- The protective plate with the smallest vertical displacement and the highest stiffness, has FE models with angles (ID 1 - 145°) and (ID 8 - 180°).
- The FE model with angle (ID 6 - 170°) exhibits the smallest value of von Mises stress for all three TNT load cases (6 kg, 8 kg, and 10 kg), demonstrating superior stress resistance.
- To achieve a more efficient configuration of protection, the development of anti-mining protection is a crucial step in the overall process of designing a complete armored vehicle.

Future research will focus on exploring various protective plate geometries, different types of high-strength steels, sandwich constructions, and composite materials to enhance the protection of troops, armored vehicles, and military equipment against the effects of Anti-Landmine Mines (ALMs) and Improvised Explosive Devices (IEDs). The ongoing research aims to optimize the safety and survivability of military personnel and equipment in hazardous environments.

**Acknowledgements:** This research is partly supported by the Ministry of Science, Technological Development and Innovation, Republic of Serbia, Agreement No. 451-03-47/2023-01/200378 and Grant TR32036.

## References

Cong M, Zhou Y, Zhang M, Sun X, Chen C, Ji C (2021). Design and Optimization of Multi-V Hulls of Light Armoured Vehicles under Blast Loads, Thin-Walled Structures, Vol. 168, 108311.

Dišić A, (2018). Development of methodology and devices for dynamic testing of materials and welded joints with application in numerical calculations of structures at high deformation rates – PhD Thesis, Faculty of Engineering, University of Kragujevac, Serbia.

Femap (2021). Finite Element Modeling and PostProcessing Application FEMAP v2021.2, Siemens.

LS-DYNA (2014). LS-PrePost-4.5-A New Post Processor for Use LSDYNA, California: Livermore.

Mahajan S, Muralidharan R (2017). Simulation of an Armoured Vehicle for Blast Loading, Defence Science Journal, Vol. 67, 449.

Markose A, Rao C.L (2017). Mechanical Response of V Shaped Plates under Blast Loading, Thin-Walled Structures, Vol. 115, 12–20.

NATO (2014). AEP-55 Procedures for Evaluating the Protection Level of Armored Vehicles – Mine Threat, NATO Standardization Agency, Vol. 2.

Pešić M, Jović N, Milovanović V, Pantić M, Živković M (2022). FE Mesh Density Influence on Blast Loading Analysis, IOP Conference Series: Materials Science and Engineering, Vol. 1271, 012016.

Pešić M, Jović N, Milovanović V, Savić D, Aničić A, Živković M, Savić S (2022). FEM Analysis of Anti-Mining Protection of Armored Vehicles, Applied Engineering Letters, Vol. 7, 89–99.

Sunil Kumar M R, Schmidova E (2019). Deformation Response of Dual Phase Steel in Static and Dynamic Conditions, Applied Engineering Letters, Vol. 4, 41–47.

Trajkovski J, Perenda J, Kunc R (2018). Blast Response of Light Armoured Vehicles (LAVs) with Flat and V-Hull Floor, Thin-Walled Structures, Vol. 131, 238–244.